13

Electron-beam modification of diffusion boride layers on the surface of 5KhNM steel

© U.L. Mishigdorzhiyn,[1] S.A. Lysykh,[1] A.S. Milonov,[1] Yu.I. Semenov,[2] M.Yu. Kosachev,[2] A.A. Starostenko,[2] V.N. Kornopol'tsev[1,3]

[1] Institute of Physical Materials Science, Siberian Branch, Russian Academy of Sciences, 670047 Ulan-Ude, Russia
[2] Budker Institute of Nuclear Physics, Siberian Branch, Russian Academy of Sciences, 630090 Novosibirsk, Russia
[3] Baikal Institute of Nature Management, Siberian Branch, Russian Academy of Sciences, Ulan-Ude, Russia
e-mail: undrakh@ipms.bscnet.ru, terwer81@mail.ru

Received April 22, 2024
Revised January 23, 2025
Accepted January 23, 2025

The present study provides results of surface hardening of samples made of the 5KhNM alloyed steel by complex saturation with boron and copper (borocoppering) to be followed by electron bean modification. The microstructure, the microhardness, the elemental and phase composition of the steel samples have been studied after complex borocoppering and subsequent electron-beam processing. It is shown that impact of the electron beam substantially increases the thickness of a boride layer, results in transition from a needle structure of the layer to a fined-grained submicron structure as well as to reduction of the microhardness and increase of layer plasticity. The X-ray diffraction analysis has revealed absence of the high-boron FeB and Cr_2B_5 phases after the electron-beam processing. The X-ray spectral microanalysis concluded that the boron content in the layer reduced from 16 to 6 wt.%, while the copper content, vice versa, increases from 2.6 to 4 wt.% along the direction from the surface.

Keywords: borocoppering, electron-beam processing,alloyed steel, microhardness, metallography, plasticity.

DOI: 10.61011/TP.2025.04.61216.139-24

Introduction

The electron-beam technologies are widely applied in metallurgy, electron microscopy, vacuum technology, microelectronics, nuclear power engineering and other industries. In particular, surface modification by the electron beam is extended to processes of thermal processing of metals and alloys as well as thin films and layers [1].

The electron-beam welders (EBW) are equipped with digitally-controlled high-accuracy deflection systems designed to move the beam on a selected area of the blank along a given contour [2]. High heating rates make it possible to shortly affect a thin surface layer of the material. In addition to welding, the EBW is also applied in quenching, annealing, tempering, texturing and polishing.

Despite a significant basis in surface modification, the effect produced by electron or laser processing is often insufficient. In aviation engineering and related fields, it is still relevant to improve strength of parts and structures which operate in extreme conditions, under joint impact of mechanical and thermal loads, agressive environment, etc. [3]. The methods of thermal-chemical treatment (TCT) of the surface of the metals and alloys such as carburizing, nitriding, boriding can largely solve this task and increase a product lifetime [4]. Thus, liquid boriding is used for hardening a wide range of products such as ploughshares, extrusion matrices, extruder screws, on-off and control valves, pump plungers, etc. [5–8]. The listed products are abrasively worn out without impact loads in conditions of agressive environments or moisture, which is explained by brittle failure susceptibility of the boride layer. It is defined by generation of stable electronic configurations in the borides sp^3 and d^5, the difference in thermal expansivities and signs of residual stresses of the FeB and Fe_2B borides [9,10]. The above-listed drawbacks are mitigated by applying various techniques of combined technologies, synthesis of the single-component Fe_2B-layer, complex saturation with boron and other element(s) [11–13]. The borocoppering is one of the TCT methods, which includes complex diffusion saturation of the surface of iron-carbon alloys with boron and copper. It has been previously established that SHS (self-propagating high-temperature synthesis) — a reaction of reduction of boron oxide together with copper oxide during boriding — promotes increase of plasticity with slight reduction of hardness and wear resistance of the generated diffusion layer based on borides [14–16].

Treatment of the metal surface with the electron or laser beam is included in advanced technologies of impact by concentrated energy fluxes (CEF, which are used for local thermal treatment of the surface [17–23]. By comparing these methods with TCT, it should be noted that the concentrated electron flux imparts its energy to the surface layer for a short period of time, which include superfast processes such as heating (the heating

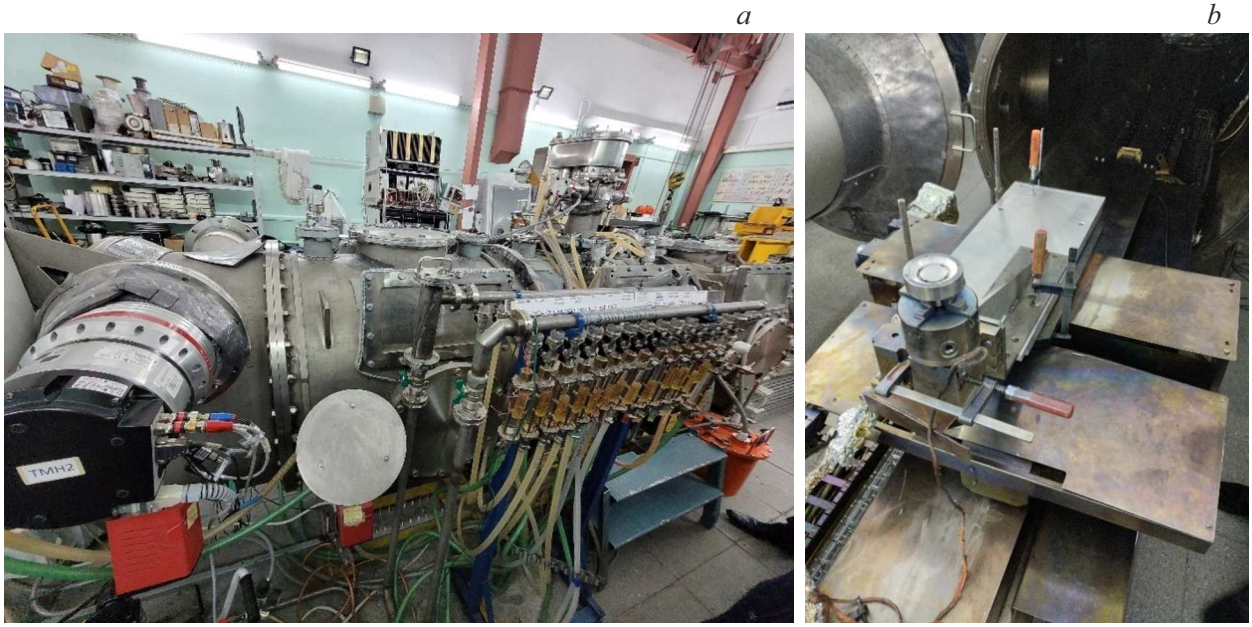

Figure 1. Experimental installation belonging to BINP SB RAS „Electron-beam technologies“: *a* — General view, *b* — Working chamber with the roll-out table.

and cooling rates of $10^5 - 10^6$ °C/s), melting, evaporation and subsequent solidification and induced dynamic stress. The listed effects render improved physical & chemical and mechanical properties to the surface layer [24]. The combined technologies of diffusion boriding with subsequent electron-beam treatment have demonstrated their efficiency in terms of brittleness reduction of the boride layer, hardness improvement and roughness reduction [13,25].

The aim of the present work is to improve the physical & mechanical properties, in particular, plasticity, while keeping high microhardness of the 5KhNM steel due to electron-beam modification of the diffusion boride layers. At the same time, the boride layers on the surface of the 5KhNM alloyed steel were produced by complex diffusion saturation with boron and copper.

1. Study methodology

The studied material was the tool die steel 5KhNM (GOST 4405-75). The 5KhNM steel is generally used for manufacturing press and hammer dies as well as inserts of matrices for horizontally-forging machines. Crazing cracks on a working surface are often a cause of failure of the dies made of this steel. Applying boriding designed, first of all, to improve wear- and corrosion resistance has demonstrated increase of the lifetime of the products made of the 5KhNM steel at least in 1.3 times in the forging and stamping industry [26–28].

The present work has the diffusion boride layers produced by borocoppering in powder mixtures containing boron carbide, copper oxide, aluminum and sodium fluoride as an activator in the following proportion: 58 %B_4C + 19 %CuO + 21 %Al + 2 %NaF. The steel surface has been diffusionally saturated in leak-tight containers in the mixture at the temperature of 1000 °C, with exposure of 4 h in a muffle furnace EKPS-50.

Then, the samples with the diffusion layers were subjected to the electron beam processing (EBP). The EBP was performed in an electron beam source belonging to BINP SB RAS (Fig. 1). Modes of processing in the electron-beam installation:

- current of the electron beam (I) – 100 mA;
- electron energy (E_i) – 60 keV;
- processing duration (t) – 1.5 s;
- electron beam diameter (d) – (10 ± 1) mm;
- pressure in the process chamber (P) – 10^{-2} Pa.

Modified layers has been metallographically analyzed on the MET 2C optical microscope. The microhardness was measured by means of the PMT-3M microhardness tester with a diamond pyramid load of 0.49 N. The elemental composition was studied in the scanning-electron microscope (SEM) JEOL JCM-6000 belonging to Research Center „Scientific Devices“ of Dorji Banzarov Buryat State University. X-ray diffraction analysis was performed in the D2 PHASER diffractometer with the LYNXEYE linear detector. The measurement step was 0.02°, while the time of one-step processing was — 1.2 s. Plasticity after complex saturation with boron and copper as well as on the samples after TCT+EBP was measured in the microhardness tester PMT-3M and the diamond pyramid load was 1.962 N. The calculation formula for determining the limit plasticity was — $\xi_{extreme} = D_{indent}/L_{crack}$ [29], where D_{indent} — a diagonal of the indent, L_{crack} — a length of the crack between the indents.

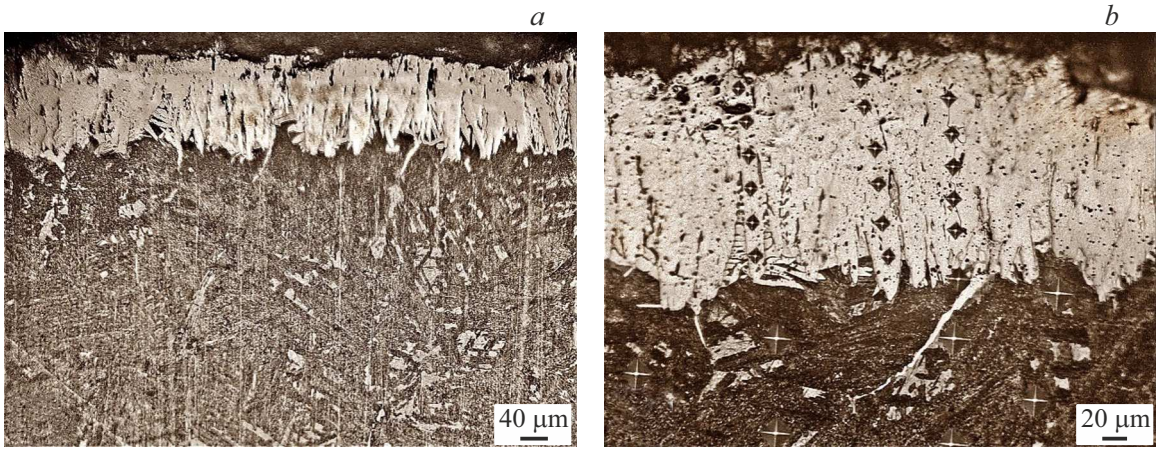

Figure 2. Microstructure of the diffusion layer of the 5KhNM steel after complex surface saturation with boron and copper: *a* — General view; *b* — Area with indents by the Vickers indenter.

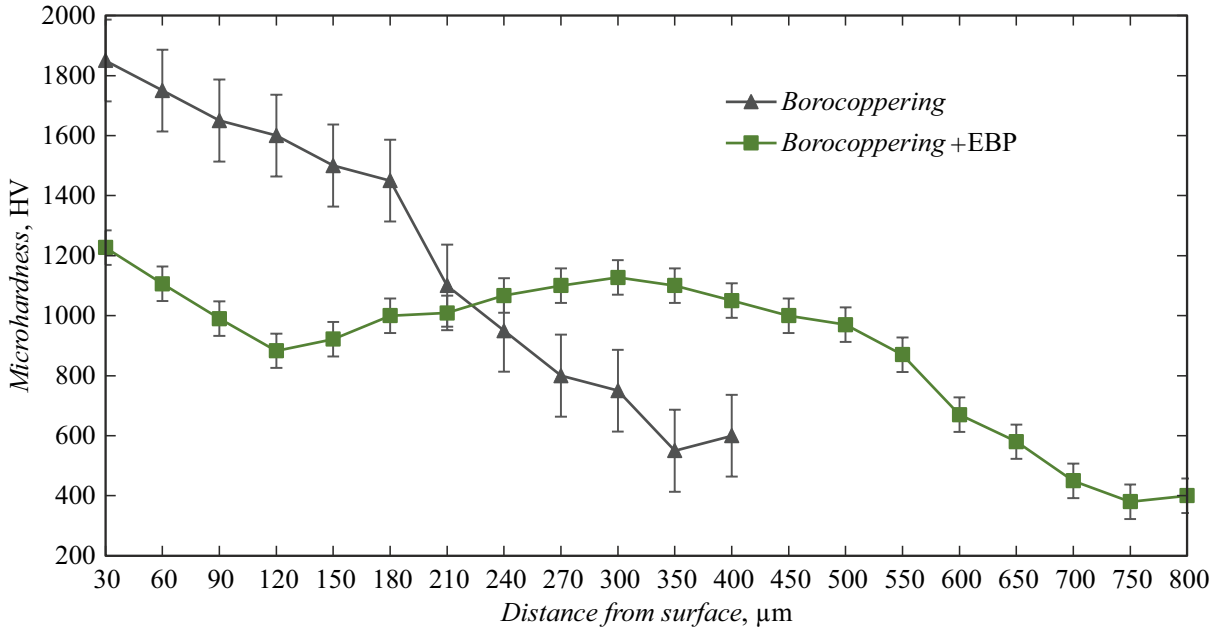

Figure 3. Distribution of microhardness on the 5KhNM steel after borocoppering and borocoppering+EBP.

2. Study results

As a result of TCT, the 5KhNM steel surface has the boride layers of the thickness 190−210 μm produced(Fig. 2).

The diffusion layer of Fig. 2 has the specific needle structure which is typical for the boride layer. The layer is compact, with the needles close to each other. The „layer"–„transition zone" interface near the base exhibits rounding of the needles with an adjacent carbo-boride phase [30]. No transition zone was revealed after etching. Microhardness in the subsurface zone (at the depth of 30 μm) is HV 1850 (Fig. 3). This value corresponds to the FeB phase after boriding of the 5KhNM steel [31]. Then, hardness was smoothly reduced to HV 1400−1500, which in turn assumes availability of the Fe_2B phase [31]. At the depth of 180−210 μm from the surface, under the basic layer there is sharp reduction of microhardness to HV 1100. In the transition zone, the microhardness is gradually reduced from HV 1100 to HV 750. The microhardness of the basic metal varied within the range HV 550−600.

The structure of the boride layer after electron beam modification is shown in Fig. 4. It is obvious that after electron beam impact the boride layer is fully transformed. The thickness of the modified layer is up to 700 μm. Fig. 4, *b* shows an upper zone of the layer, which after etching had got a light metallic color. The thickness of this zone was

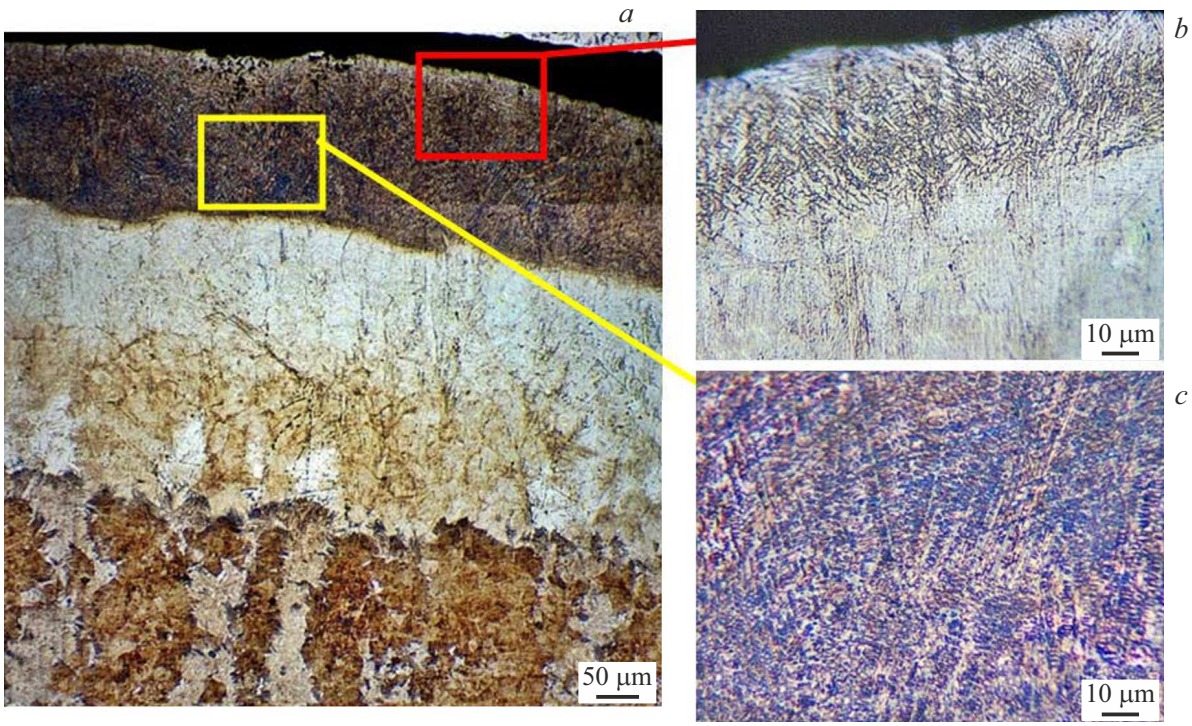

Figure 4. Microstructure of the borated 5KhNM steel after electron beam modification: *a* — General view; *b* — the subsurface zone; *c* — the eutectic zone.

40–60 μm. The micro structure consists of the needle eutectic with the maximal microhardness of HV 1227 (Fig. 3). In the depth of this zone at the distance of 160–200 μm from the surface the eutectic structure exhibits more clearly (Fig. 4, *c*). Microhardness inside this area is within the range HV 920–1000.

Below to the base border there is the most extensive (in terms of the depth) zone of the thickness 400–450 μm. After etching this area has got light tones, while the „layer"–„base" interface exhibits bright light flaky inclusions. Microhardness in this zone increases somewhat to HV 1100 at the depth of 300 μm from the surface. Further on, microhardness is smoothly reduced to HV 450 at the border with the basic metal (Fig. 3).

The maximal microhardness of the boride layer after EBP is reduced in 1.5 time from HV 1850 to HV 1227, which is related to changing of the phase composition in the subsurface layers, in accordance with the results of X-ray diffraction analysis below in the text. Reduction of microhardness to the values HV 1200–1500 in case of boriding is often a positive factor, which can reduce high brittleness of the layer. For these purposes, there are various techniques for producing the boride layer with predominant generation of the more plastic Fe_2B phase [32–34]. Increased plasticity of the boride layers makes it possible to extend the application field, including in conditions of impact loads.

The microhardness profiles are different before and after EBP. Usually, after traditional boriding microhardness is steadily reduced from the surface to the base, which is also true for borocoppering [9,16]. After EBP, the modified boride layer has cycle variation of microhardness from HV 1227 at the surface to HV 883 at the depth of 120 μm. In the central zone of the layer microhardness is again reduced to HV 1100 and then it is gradually reduced when getting to the basic metal.

The electron beam significantly affects the microstructure of the 5KhNM steel (Fig. 5). After borocoppering, the steel microstructure consists of laminar perlite with ferrite inclusions (light inclusions) (Fig. 5, *a*). Fig. 5, *b* shows the microstructure of the 5KhNM steel after impact by the electron beam. The laminar perlite becomes a grainy one, while the ferrite volume is increased and generates solid vertical agglomerates.

The elemental composition from the 5KhNM steel after TCT has been analyzed to show that the largest content of boron is observed at the sample surface and is 16.43 wt.%, thereby corresponding to the FeB phase (Fig. 6, *a*, Table 1) [16]. Further on, its content is gradually reduced towards the base. The content of the alloying elements Cr, Mo, Ni in the layer approximately corresponds to their content in the 5KhNM except for the last element, whose content in the layer is in two times lower than in the base. Probably, Ni is pushed by diffusing elements — boron and copper and by iron borides being generated as well. The greatest content of copper is detected on the layer surface and it is 2.6 wt.%. It significantly exceeds the solubility limit of copper in α-iron and the FeB boride, thereby indicating

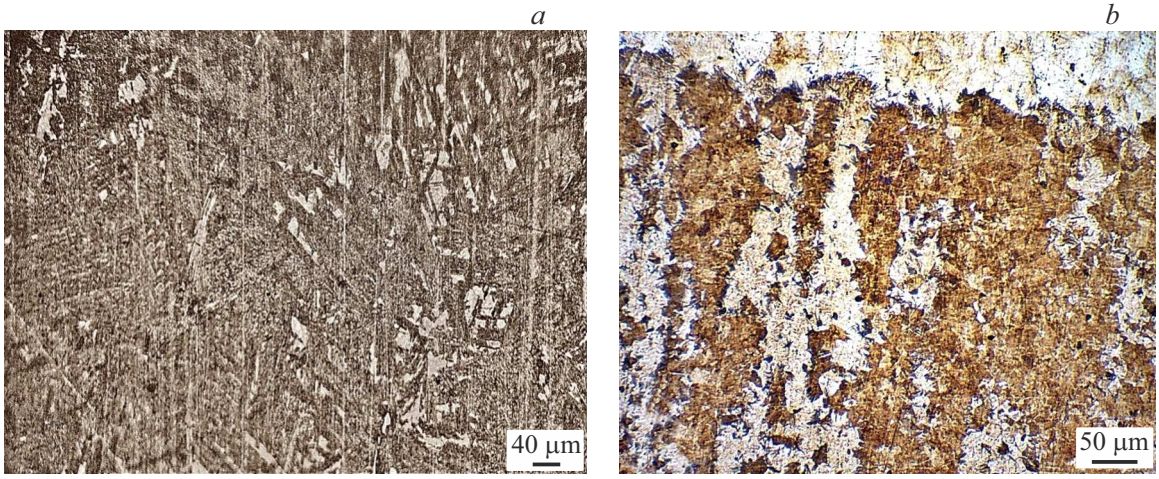

Figure 5. Microstructure of the 5KhNM steel under the boride layer: *a* — after TCT, *b* — after TCT+EBP.

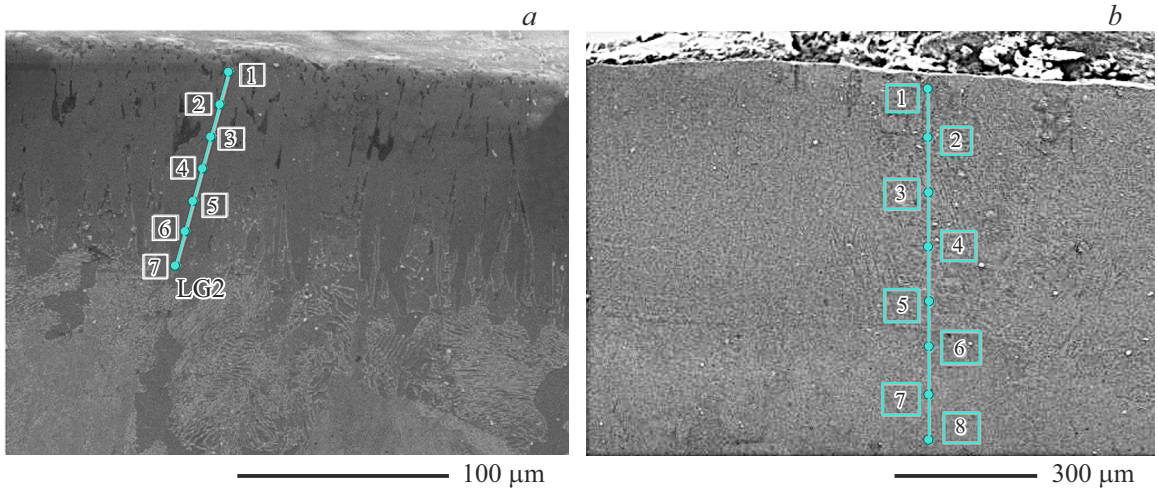

Figure 6. Microstructure of the 5KhNM steel after borocoppering with spectrum take-off points during the elemental analysis: *a* — after TCT; *b* — after TCT+EBP.

Table 1. Elemental composition of the diffusion layer on the 5KhNM steel after TCT

Spectrum points	Chemical elements, wt.%							
	B	C	Al	Cr	Ni	Cu	Mo	Fe
1	16.43	0.35	0.3	0.66	0.67	2.6	0.57	78.42
2	14.77	0.15	0.51	0.66	0.67	–	0.14	83.1
3	12.05	0.06	–	0.53	0.51	0.51	0.27	86.07
4	5.98	0.03	–	0.62	0.31	–	0.34	92.72
5	1.35	0.41	–	0.63	0.46	–	0.25	96.9
6	0.21	0.37	0.56	0.59	0.57	0.09	0.07	97.54
7	–	0.4	0.58	0.4	0.56	0.54	–	97.52

Table 2. Elemental composition of the diffusion layer on the 5KhNM steel after TCT+EBP

Spectrum points	Chemical elements, wt.%							
	B	C	Al	Cr	Ni	Cu	Mo	Fe
1	1.43	1.35	0.14	0.63	–	–	4.06	92.39
2	0.87	2.63	0.36	1.28	–	1.61	2.77	90.48
3	3.48	2.56	0.51	1.23	–	0.32	2.62	89.28
4	4.01	2.38	0.43	1.5	0.15	–	6.69	84.84
5	3.46	1.94	0.54	1.33	0.39	–	2.99	89.35
6	5.38	1.8	0.74	–	–	3.99	1.18	86.91
7	6.22	2.27	1.15	1.1	–	–	3.1	86.16
8	6.34	2.09	0.67	0.16	1.03	4.02	3.3	82.39

its presence in a free form [35,36]. The layer exhibits a small content of aluminum — up to 0.58 wt.%, which is contained in the initial saturating mixture.

The distribution of the elements after electron-beam impact differs from that after TCT. The boron concentration increases towards the base. At the same time, its maximum content — 6.34 wt.% — is detected at the interface of the basic metal (Fig. 6, *b*, Table 2). The copper content also increases as moving away from the surface and is 4.02 wt.%. The concentrations of the alloying elements Cr, Mo, Ni varies stepwise after EBP. Thus, for Cr and Ni the values oscillate from zero to 1.5 and to 1.03 wt.%, respectively. The molybdenum content varies from 1.18 to 6.69 wt.%, which significantly exceeds its content in the initial steel. It shall be noted that the maximum content of Cr and Mo is recorded at the depth of about 300 μm from the surface. This allows us to assume that increase of microhardness in the central area of the layer is related to the high content of the said carbide-generating elements. The curve of the boron content vs. the layer depth clearly demonstrates variation of the boron concentration after EBP (Fig. 7). Redistribution of the boron atoms under electron impact is probably related

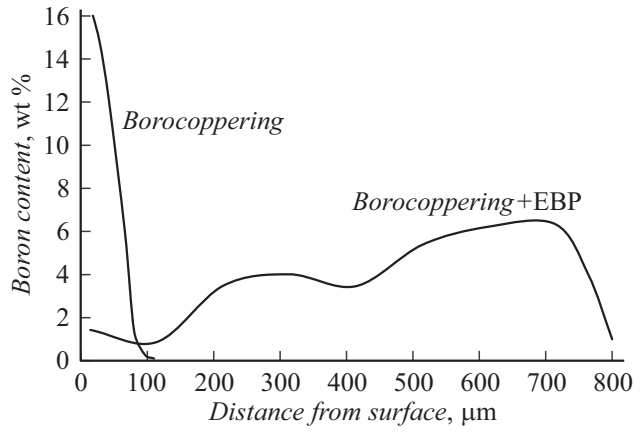

Figure 7. Variation of boron concentration along the layer depth before and after EBP on the 5KhNM steel.

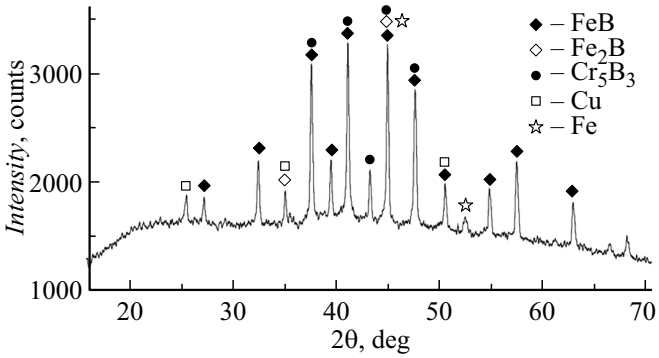

Figure 8. XRD pattern of the 5KhNM steel sample after borocoppering.

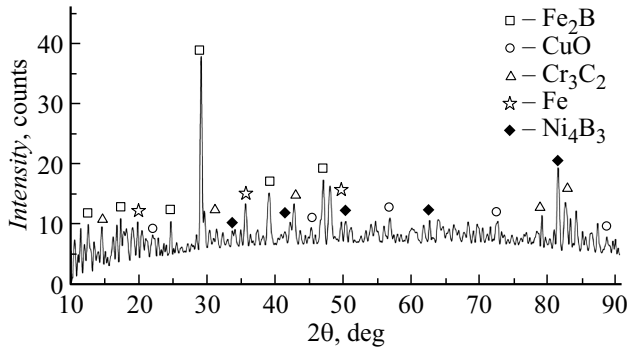

Figure 9. XRD pattern of the 5KhNM steel sample after borocoppering and EBP.

to remelting and mixing processes in the subsurface layers which contribute to uniform distribution of the element concentrations including boron. Besides, as a result of elastic interaction of electrons from the external source with crystal lattice of the borides there is displacement of the boron atoms with the least atomic weight to distances which significantly exceed interatomic distances, along the motion direction of the electron flux.

The XRD of the sample after TCT exhibits presence of three borides: FeB, Fe_2B and Cr_7B_5 (Fig. 8). Copper and

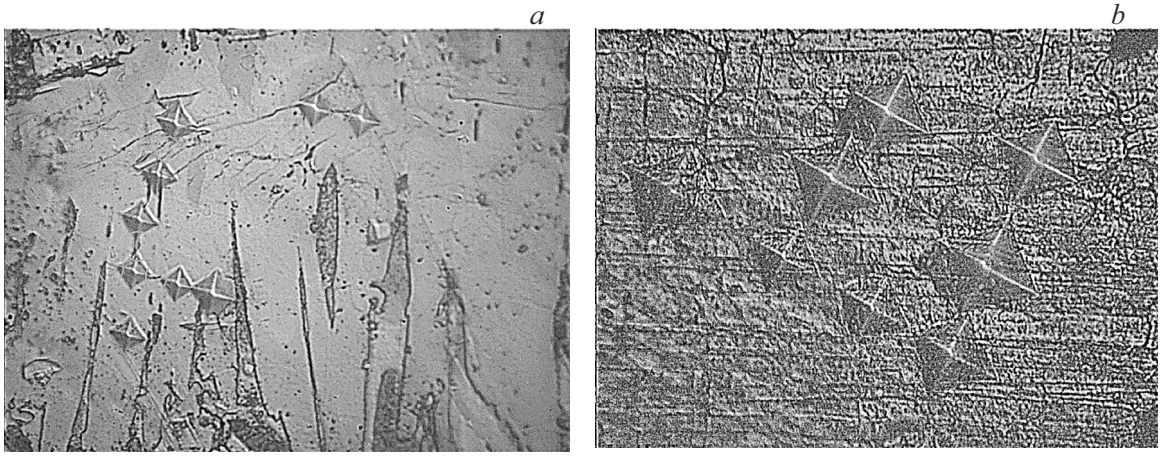

Figure 10. Microstructure of the 5KhNM steel when measuring the limit plasticity: *a* — after TCT; *b* — after TCT+EBP.

iron are found in a pure form, thereby confirming the results of the elemental analysis and the previous studies [37].

The EBP has resulted in changing of the phase composition of the boride layer on the 5KhNM steel. Specifically, only two borides are detected. Fe_2B and Ni_4B_3 (Fig. 9). The high-boron FeB phase is not detected as the previously detected boron concentration is insufficient for its generation. Besides, chrome carbide Cr_3C_2, bivalent copper oxide CuO and α-iron are detected.

Fig. 10 shows micropictures of the boride layers with the indents of the diamond indenter. Presence of cracks between the indents indicates brittleness (plasticity) of the diffusion layer before and after EBP. After borocoppering, the limit plasticity as calculated by the formula of work [29] was 1.79; 2.19; 2.08; 2.18 points. It is known that after borocoppering the average value of the limit plasticity is 1.13−1.20, which in 1.5−2 times lower than after borocoppering [15]. After exposing the diffusion layer with the electron beam, no crack between the indents is detected. Its absence makes it impossible to evaluate a brittleness point of this type of the layers as per the Skudnov formula. It is obvious that the modified layer significantly exceeds the initial boride layer in terms of plasticity.

Conclusion

1) after complex borocoppering the thickness of the boride layer on the surface of the 5KhNM steel sample was 190−210 μm. Subsequent impact by the electron beam allowed to increase the layer thickness to 650−700 μm;

2) irradiation by the electron beam resulted in significant changes of the structure & phase state of the boride layer. The needle structure of the initial layer was mitigated, and instead the dispersed eutectic structure with more plastic borides was formed;

3) processing of the surface with the electron beam contributes to reduction of maximum microhardness and increase of the limit plasticity as compared to TCT;

4) it has experimentally determined the EBP parameters ($I = 100$ mA, $E_i = 60$ keV, $t = 1.5$ s), which result in remelting of the diffusion boride layer without altering the sample geometry.

Funding

The works for the chemical-thermal processing and the structure & phase studies were supported financially under the government task of the RF Ministry of Science and Higher Education, research topic FWSF-2024-0010. The works for the electron-beam processing were supported financially under the government task of the RF Ministry of Science and Higher Education, research topic FWGM-2022-0008.

Conflict of interest

The authors declare that they have no conflict of interest.

References

[1] Z. Shiller, U. Gaizig, Z. Pantsenr. *Electronno-luchevaya tekhnologia* (Energiya, M., 1980) (in Russian)

[2] O.N. Alyakrinskii, M.A. Batazova, D.Yu. Bolkhovityanov, M.Yu. Kosachev, P.V. Logachev, A.M. Medvedev, Yu.I. Semenov, M.M. Sizov, A.A. Starostenko, A.S. Tsyganov. Nauchnoe priborostroenie, **29** (1), 26 (2019). (in Russian) DOI: 10.18358/np-29-1-i2632

[3] V.I. Butenko, A.D. Zakharchenko, D.S. Durov, R.G. Shapovalov, T.A. Rybinskaya, V.N. Podnozhkina. Izvestiya YuFU. Tekhnicheskie nauki (Spetsialnyi vypusk), **78** (1), 198 (2008). (in Russian)

[4] L.G. Voroshnin, O.L. Mendeleeva, V.A. Smetkin. *Teoriya i technologiya khimiko-termicheskoi obrabotki* (Novoe znanie, Minsk, M., 2010) (in Russian)

[5] S.G. Tsikh, V.N. Martynov, N.E. Shklyar. Ritm, **6**, 38 (2015). (in Russian)

[6] A.A. Krasulya, U.L. Mishigdorzhiin, N.S. Ulakhanov, A.G. Tikhonov, A.S. Pyatykh, K.A. Demin. Uprochnyayushchie tekhnologii, **20** (1), 26 (2024). (in Russian) DOI: 10.36652/1813-1336-2024-20-1-26-31
[7] A.A. Krasulya, A.S. Pomelnikova, K.O. Bazaleeva, A.V. Zavodov, E.V. Tsvetkova, S.G. Tsikh. Tekhnologiya metallov, **1**, 2 (2022). (in Russian) DOI: 10.31044/1684-2499-2022-0-1-2-8
[8] A.A. Krasulya, A.A. Permitina, A.S. Pomelnikova, S.G. Tsikh. Zagotovitelnye proizvodstva v mashinostroenii, **19** (9), 419 (2021). (in Russian) DOI: 10.36652/1684-1107-2021-19-9-419-421
[9] M.G. Krukovich, B.A. Prusakov, I.G. Sizov. *Plastichnost' borirovannykh sloev* (Fizmatlit, M., 2010) (in Russian)
[10] Z. Pala, J. Fojtikova, T. Koubsky, R. Musalek, J. Strasky, J. Capek, J. Kyncl, L. Beranek, K. Kolarik. Powder Diffraction, **30** (1), 83 (2015). DOI: 10.1017/S0885715615000019
[11] A. Bartkowska, D. Bartkowski, D. Przestacki, J. Hajkowski, A. Miklaszewski. Coatings, **11**, 608 (2021). DOI: 10.3390/coatings11050608
[12] F. Xie, X.J. Wang, J.W. Pan. Vacuum, **141**, 166 (2017). DOI: 10.1016/j.vacuum.2017.04.011
[13] R. Zenker. *Electron Beam Surface Technologies*. In Encyclopedia of Tribology, ed. by Q.J. Wang, Y.W. Chung (Springer, Boston, MA, USA, 2013), DOI: 10.1007/978-0-387-92897-5_723
[14] S.A. Lysykh, U.L. Mishigdorzhiin, Yu.P. Kharaev, P.V. Moskvin, M.S. Vorobiev, M.A. Mokeev. Polzunovskii vestnik, **2**, 217 (2023). (in Russian) DOI: 10.25712/ASTU.2072-8921.2023.02.028
[15] S.A. Lysykh, V.N. Kornopoltsev, Kh.S. Chzhun, B.D. Lygdenov, A.M. Guriev. Polzunovskii vestnik, **3**, 77 (2020). (in Russian) DOI: 10.25712/ASTU.2072-8921.2020.03.014
[16] L.G. Voroshnin. *Borirovanie promyshlennykh stalei i chugunov, sprav.* posobie (Belarus', Minsk, 1981) (in Russian)
[17] V.I. Itin, B.A. Koval', N.N. Koval'. Izvestiya vuzov. Fizika, (in Russian) **6**, 38 (1985).
[18] Y.F. Ivanov, V.P. Rotshtein, D.I. Proskurovsky, P.V. Orlov, K.N. Polestchenko, G.E. Ozur, I.M. Goncharenko. Surf. Coat. Technol., **125** (1−3), 251 (2000). DOI: 10.1016/S0257-8972(99)00569-1
[19] V.A. Gribkov, F.I. Grigoriev, B.A. Kalin, V.L. Yakushin. *Perspektivnye radiatsionno-puchkovye technologii obrabotki metallov* (Kruglyi god, M., 2001) (in Russian)
[20] Yu. Ivanov, W. Matz, V. Rotshtein, R. Günzel, N. Shevchenko. Surf. Coat. Technol., **150** (2−3), 188 (2002). DOI: 10.1016/S0257-8972(01)01542-0
[21] V. Engelko, B. Yatsenko, G. Mueller, H. Bluhm. Vacuum, 62 (2-3), 211 (2001). DOI: 10.1016/S0042-207X(00)00446-2
[22] V.E. Ovcharenko, S.G. Psakh'e, D.I. Proskurovskii, G.E. Ozur. (Pat. RF, № 2259407, 2259407 C1, C21D 9/22, 1/09, 2005) (in Russian)
[23] I.M. Goncharenko, V.I. Itin, S.V. Isichenko, S.V. Lykov, A.B. Markov, O.N. Nalesnik, G.E. Ozur, D.I. Proskurovskii, V.P. Rotshtein. Zashchita metallov, **29** (5), 18 (1993). (in Russian)
[24] Sh. Hao, Bo Gao, A. Wu, J. Zou, Yi. Qin, Ch. Dong, J. An, Q. Guan. Nucl. Instrum. Methods Phys. Res. Section B: Beam Interactions with Mater. Atoms, **240** (3), 646 (2005). DOI: 10.1016/j.nimb.2005.04.117
[25] N.S. Ulakhanov, U.L. Mishigdorzhiin, A.P. Semenov, A.S. Milonov, M.S. Vorobiev, P.V. Moskvin, V.I. Shin. Vestnik Sibirskogo gos. industrial'nogo un-ta, **1** (47), 92 (2024). (in Russian) DOI: 10.57070/2304-4497-2024-1(47)-92-102
[26] Yu.P. Kharaev, A.D. Greshilov, L.A. Kurkina, N.I. Fedotov, V.A. Butukhanov. Obrabotka metallov (tekhnologiya, oborudovanie, instrumenty), (in Russian) **2** (55), 62 (2012).
[27] R.A. Vikhrev, I.P. Polyanskii, I.G. Sizov. Sovremennye materialy, tekhnika i technologii, **4** (43), 28 (2022). (in Russian) https://www.elibrary.ru/item.asp?id=49957662
[28] M.V. Sitkevich. Tez. dokl. *Respublikanskaya nauchno-tekhnicheskaya conferentsiya professorsko-prepodavatel'skogo sostava, nauchnykh rabotnikov, doktorantov i aspirantov MTF BNTU* (Minsk, Belarus', (in Russian) 2022), P. 67. https://rep.bntu.by/handle/data/132203
[29] V.A. Skudnov. *Predel'nye plasticheskie deformatsii metallov* (Metallurgiya, M., 1989) (in Russian)
[30] M.G. Krukovich. Evraziiskii Soyuz Uchenykh (ESU), **10** (79), (in Russian) 30 (2020). DOI: 10.31618/ESU.2413-9335.2020.6.79.1075
[31] D. Sánchez Huerta, N. López Perrusquia, I. Hilerio Cruz, M.A. Doñu Ruiz, E.D. García Bustos, M. Flores Martínez. Defect and Diffusion Forum, **380**, 29 (2017). DOI: 10.4028/www.scientific.net/ddf.380.29
[32] H. Nakajo, A. Nishimoto. J. Manufacturing and Mater. Process., **6** (2), 29 (2022). DOI: 10.3390/jmmp6020029
[33] E. Mertgenç, Y. Kayali. Canadian Metallurgical Quarterly, **62** (2), 362 (2023). DOI: 10.1080/00084433.2022.2082203
[34] F. Xie, X.-J. Wang, J.-W. Pan. Vacuum, **141**, 166 (2017). DOI: 10.1016/j.vacuum.2017.04.011
[35] J. Miettinen, V. Ville-Valtteri, T. Fabritius. Archives of Metallurgy and Materials, **66** (1), 297 (2021). DOI: 10.24425/amm.2021.134787
[36] V.I. Alekseev, V.A. Ivoditov, V.S. Yusupov. Perspektivnye materialy, **4**, 13 (2008). (in Russian).
[37] V. N. Kornopol'tsev Polzunovskii vestnik, **1**, 135 (2012) (in Russian).

Translated by M.Shevelev